Effect of Inlet Additive Drag on Aircraft Performance

Joseph S. Mount*
North American Aviation, Inc., Los Angeles, Calif.

The percentage of the theoretical additive drag (D_{ADD}, the force associated with spilling excess air around a jet engine inlet) that may be recovered as a change in the pressure drag of the inlet cowl is discussed. It is shown that, for "off-design" operation, D_{ADD} can be a significant percentage of the total airplane drag. An additive drag correction factor K_{ADD} is defined such that the drag force felt by the vehicle equals ($K_{ADD} \times D_{ADD}$). The effect of K_{ADD} on typical aircraft missions is presented. Miscellaneous test results are shown to substantiate the K_{ADD} values used. A model wind-tunnel program aimed specifically at getting systematic additive drag data is described, and first phase test results are presented.

Nomenclature

A = area, ft^2
C_P = pressure coefficient, $(P - P_0)/q_0$
D = diameter, in. (hydraulic diameter for noncircular cross-section)
D = drag force, lb
D_{ADD} = theoretical additive drag, as defined in Figs. 1, 2, and 3 (generalized data is plotted in Ref. 5)
D_{AUX} = drag of air taken aboard but extracted for auxiliary purposes such as compartment cooling and boundary-layer control
D_{BP} = drag of bypass air (if required for engine matching)
F_G = gross thrust of jet nozzle = $(W/g)V_e + (P_e - P_0)A_e$
F_N = net thrust = $F_G - (W/g)V_0$
K_{ADD} = additive drag correction factor = $[D_{ADD_{Theo}} - (\text{Forebody Drag}_{MFR>1.0} - \text{Forebody Drag}_{MFR=1.0})]/D_{ADD_{Theo}}$
M = Mach number
MFR = inlet mass-flow-ratio = A_0/A_{LE} for pitot and axisymmetric inlets; A_0/A_c for supersonic ramp inlets
$\bar{P}$ = average pressure
r = lip radius, in.
$TOGW$ = takeoff gross weight, lb
V = velocity, fps
w = ramp width, supersonic inlet
W = mass-flow-rate, lb/sec
X = cowl length, to point of tangency to axis of symmetry
θ = net turning angle at inlet station, deg
δ = incremental turning angle, deg

Subscripts

0 = freestream
1 = inlet lip station
c = projected capture area defined by cowl lip and ramp leading edge
e = jet nozzle exit conditions
LE = projected cross section at tip of lip leading edge
MAX = maximum external cross section of forebody
MIN = minimum area throat of inlet
P = projected
R = ramp (two-dimensional inlet)
S = spike (axisymmetric inlet)

Definitions

INLET additive drag is the force exerted in the thrust direction on the streamtube of air entering the inlet of an air-breathing engine by the surrounding atmosphere. The mathematical expression is obtained by summing the x-direction forces algebraically and setting them equal to the x-direction change in momentum. The fluid flow situation is illustrated in Figs. 1–3 for a pitot-type inlet, supersonic two-dimensional inlet, and supersonic spike inlet, respectively. This theoretical additive drag is a mathematical term that gets into the equation for the net propulsive effort (F_{NE}) exerted on a vehicle by the internal air because it is convenient to work to a freestream condition in computing installed engine performance.

$$F_{NE} = F_N - (D_{ADD} \times K_{ADD}) - D_{BP} - D_{AUX}$$

where

$$F_N = F_g - (W/g)V_0$$

and K_{ADD} = an empirical multiplying factor (other terms as noted in the Nomenclature).

The theoretical additive drag would always be zero if the inlet geometry were so completely flexible that the inlet capture area always exactly matched the streamtube area demanded by the engine and auxiliary systems. Generally, supersonic inlets are designed to have the term very close to zero at the maximum design Mach number. At off-design Mach numbers and at reduced power conditions, additive drag appears and must be considered as a quantity to be traded against inlet complexity and bypass drag.[2]

Off-Design Conditions

The more off-design conditions (from the inlet point of view) that appear as prime operating points for the vehicle, the larger effect additive drag will have on vehicle capability. The off-design condition is usually typified by the engine's demand for air, as expressed in terms of freestream tube area, being considerably less than the inlet can capture, i.e., a low mass-flow condition. Examples of off-design conditions for specific types of vehicles are as follows:

Supersonic transport: 1) Transonic acceleration at high enough altitude to avoid unacceptable sonic booms (this condition will establish engine size), 2) Subsonic cruise for secondary leg of split route, 3) Maximum economy hold.

V/STOL transport: 1) Subsonic cruise at reduced power with fan-type engines of large air handling capacity sized for lifting.

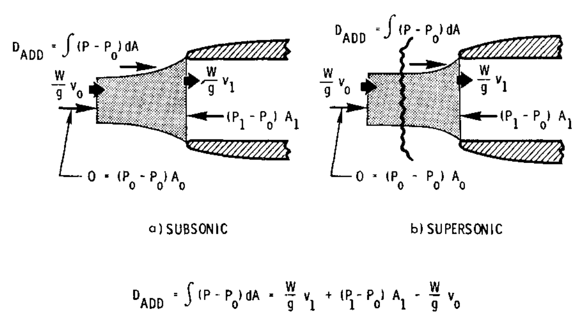

Fig. 1 Additive drag of a pitot inlet.

Presented as Preprint 64-599 at the AIAA Transport Aircraft Design and Operations Meeting, Seattle, Wash., August 10–12, 1964; revision received February 25, 1965.

* Supervisor, Internal Aerodynamics, Los Angeles Division. Member AIAA.

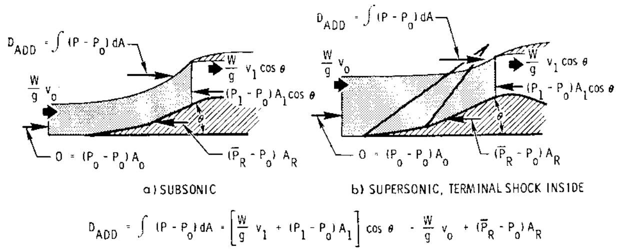

Fig. 2 Additive drag of a two-dimensional inlet.

ASW: 1) Low-speed search after a long high-speed (subsonic) run to station.

Strategic and tactical penetrators: 1) Extended transonic or high-subsonic low-altitude penetration with inlets and engines capable of adequate supersonic performance, 2) rate-of-climb transonically to effectively accomplish alternate supersonic missions.

Effect on Performance

As a quantitative example of how theoretical additive drag compares to zero-trim aircraft drag, Figs. 4 and 5 have been prepared. The solid lines represent nondimensionalized zero-trim drag for an SST and for a V/STOL transport. The solid dots represent the total drag level for the operating points described if the full theoretical additive drag were to be felt by the vehicle. The asterisks are indicative of the reduction in the theoretical additive drag that is obtainable by present state-of-the-art shaping of the inlet lips, as obtained from the test data to be discussed. Similar breakdowns could be shown for other vehicles and should, as a matter of fact, be made a part of the design development procedure for any study vehicle. Figure 6 is a summary of what additive drag would mean to off-design vehicle performance if the entire theoretical additive drag term were to actually appear as a drag force on the vehicle. The asterisks in this figure again indicate the reduction in the theoretical additive drag penalty when the appropriate "best estimate" K_{ADD} is applied.

Reduction of Losses

Of course, in approaching a propulsion design problem, the inlet is always sized and matched to the engine with considerable attention directed toward keeping the theoretical additive drag low. (This was done for the examples given.) In addition, engine cycle changes should be considered which match the engine to the inlet. Far beyond the normal high- and low-flowing and bypass-ratio changes available for a given engine is the completely flexible variable-pumping-compressor concept, which has been pioneered by the Research and Technology Development (R&TD) Propulsion Laboratory at Wright Field. All of these changes bear penalties of added

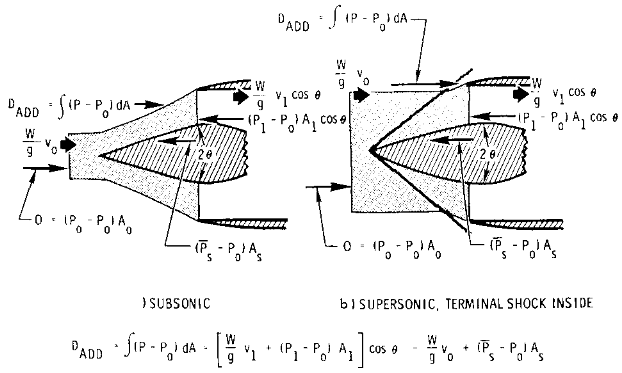

Fig. 3 Additive drag of a spike inlet.

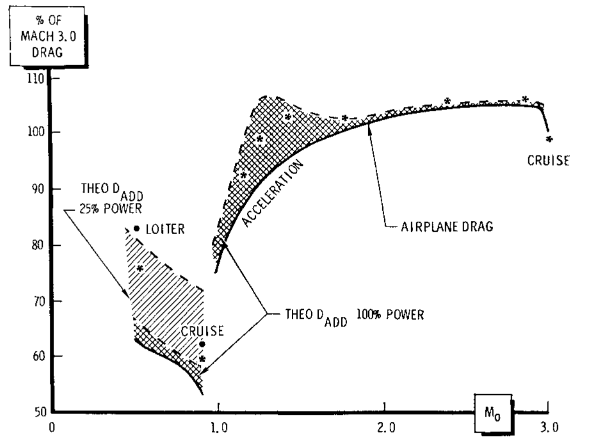

Fig. 4 Theoretical D_{ADD} and (D_{ADD} and K_{ADD}) on an SST.

control complexity, cost, and weight. Also, in general, they bear penalties of increased specific fuel consumption and of reduced reliability because of the complexity.

Operating the inlet at maximum mass-flow-ratio through the use of a bypass system usually is profitable for supersonic designs, although the weight, control complexity, and drag of this system must be balanced against the reduced additive drag.

It has long been realized[4,7] that the theoretical additive drag is not always entirely manifested as a drag force on the vehicle. Because of lip suction forces[3,6] and physical departures from an inviscid flow situation, the drag of the inlet forebody often will not increase by the full amount of the theoretical additive drag as mass-flow-ratio is decreased. From a bookkeeping standpoint, this may be thought of most conveniently as a cancellation of part of the theoretical additive drag. The most convenient way to express this cancellation is in the form of a multiplying correction factor to the theoretical additive drag term, such that the actual drag force felt by the vehicle is ($D_{ADD} \times K_{ADD}$).

Additive Drag Correction Factor

This correction factor K_{ADD} will obviously be a function of inlet type and geometry and of lip contour, as well as of the aerodynamic parameters of Mach number and mass-flow-ratio. It is generally recognized that K_{ADD} can be minimized by certain types of contouring of lips and forebodies. To the author's knowledge, although some published material has explored the concept of additive drag cancellation (e.g., Refs.

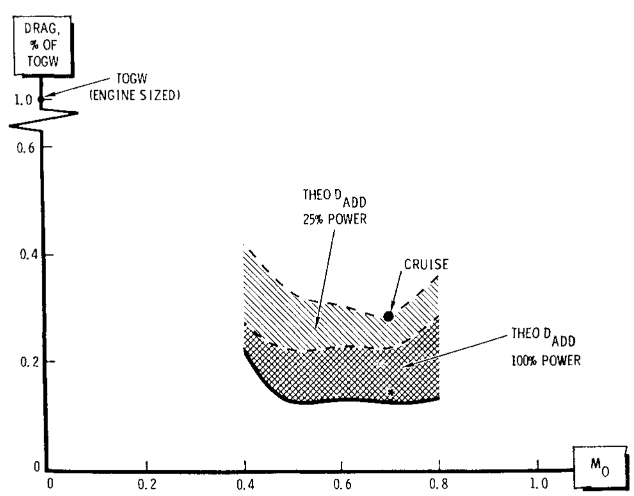

Fig. 5 Theoretical D_{ADD} and (D_{ADD} and K_{ADD}) on a V/STOL transport.

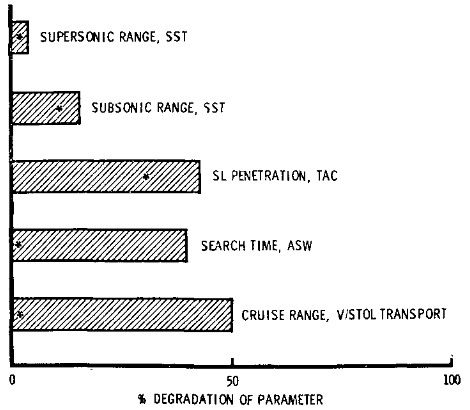

Fig. 6 Mission penalties for drag increase of 100% theoretical D_{ADD} and for "best estimate" ($D_{ADD} \times K_{ADD}$).

1, 4, 7, 8, 10), there has been no systematic attempt to investigate the effect of the variables involved on a built-for-the-purpose model. This appears to be one of the many little technical pockets that has been skipped over in the transition from high-speed subsonic to supersonic design-point flight. It is one that merits additional experimental effort now that significant off-design capability must be built into supersonic machines and into V/STOL type machines whose lift-cruise engine installations must be sized for the lifting job and which will operate at reduced power setting for cruise.

Existing Data

A correlation was made of available wind-tunnel test data for ducted models. Much of the source material is of relatively ancient origin. Of course, it cannot be claimed that all existing pertinent material was included. Indeed, it seems likely that a great deal of additional data (both published and unpublished) must exist in the industry, which could be used profitably to extend this work.

The configurations studied were, for the most part, pitot-type subsonic and transonic models. A small amount of data were available from a Mach 2.0, external compression, wedge inlet model.[4] No relevant results for axisymmetric supersonic inlets were found.

Even at its best, this type of correlation produces results of limited usefulness. The models and test programs were directed to purposes other than measuring additive drag cancellation. Some had wings and forebodies, which gave high base-point drag levels and which tended to obscure drag changes with mass-flow-ratio. Inlet contours were often quite configuration-oriented and were not varied in a methodical way. Mach number and mass-flow-ratio coverage was spotty.

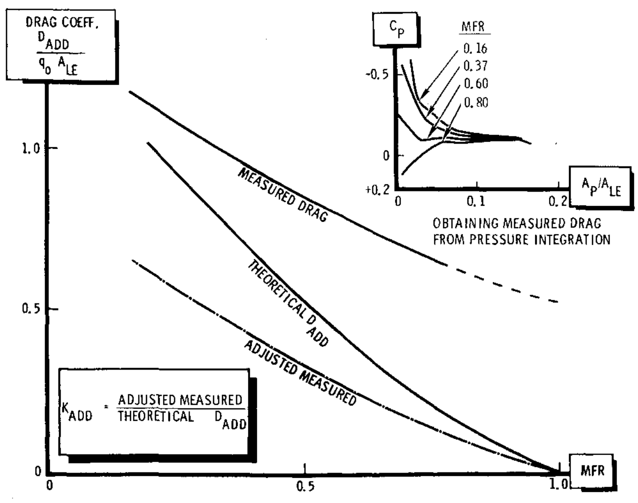

Fig. 7 Obtaining K_{ADD} from model.

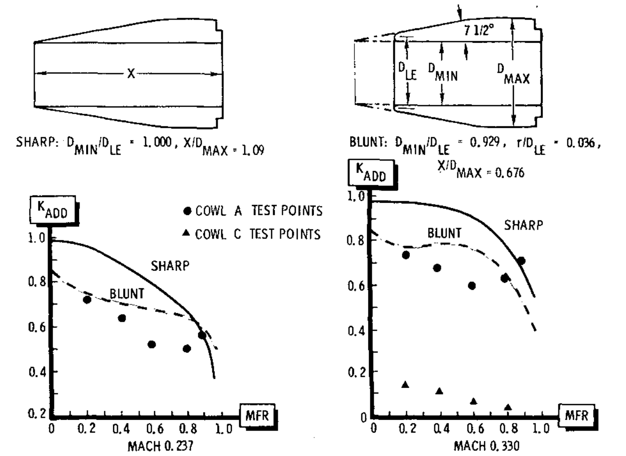

Fig. 8 Mach 0.237 and 0.330 tests. Effect of lip blunting. Round pitot inlets. NACA TN 3170. Force model (D_{MIN}/D_{MAX} = 0.755).

Curves of K_{ADD} were obtained from two different types of models, force and pressure, which required two different approaches to data handling. One involved recording drag balance measurements while varying inlet mass-flow-ratio and plotting the results on coordinates of drag coefficient vs mass-flow-ratio as in Fig. 7. The measured drag was then adjusted to zero at MFR = 1.0, as shown, and compared with the theoretical additive drag. The ratio of this adjusted measured drag to the theoretical additive drag is then K_{ADD}.

The second case involved models that had extensive external lip pressure instrumentation. With these models, the pressure distribution was plotted against the area perpendicular to the duct centerline (see insert, Fig. 7) upon which it must act to produce a force in the drag direction. These plots were next integrated for each mass-flow-ratio tested. The resulting force was plotted, as before, on coordinates of drag coefficient vs mass-flow-ratio and adjusted to zero at MFR = 1.0. Since these are suction (thrust) forces, they are subtracted from the theoretical additive drag curve to give the "adjusted measured" drag by this method. The ratio of this "adjusted measured" drag to the theoretical additive drag again defines K_{ADD}.

Because of the lack of coverage of variables, it was decided to build and test a series of "typical" inlets to compare with the existing data and to fill in the gaps. The results of some of the literature correlations are shown in Figs. 8–11. Figures 8 and 9 present a general picture of K_{ADD} for pitot inlets at low subsonic Mach numbers, whereas Figs. 10 and 11 present K_{ADD} data for a two-dimensional supersonic inlet. Much cross-plotting and fairing was necessary to produce smooth curves. Data points from similar configurations from the present test program are spotted on Figs. 8 and 9 for comparison purposes.

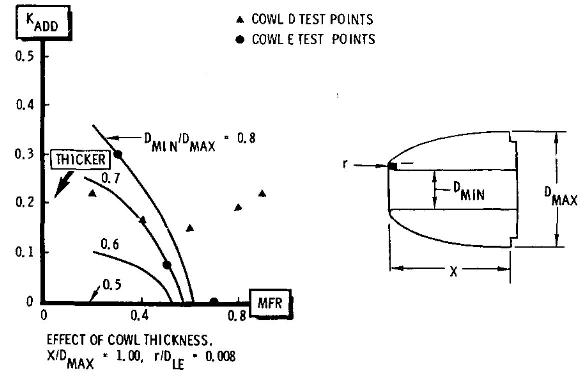

Fig. 9 Mach 0.4 tests. NACA Series 1 round pitot inlets. Rept. 920. Pressure model.

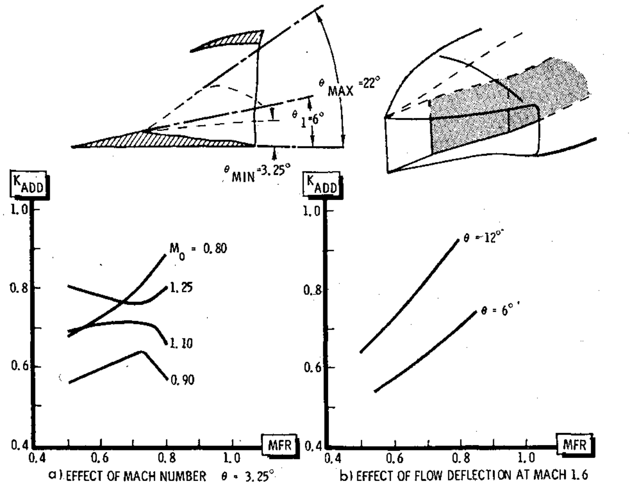

Fig. 10 Mach 0.80–1.60 tests. Two-dimensional ramp inlet. NA-64-363. $W/A_c = 0.029$, $r/D_c = 0.002$.

The force model of Fig. 8 shows that, for a $7\frac{1}{2}°$ conical cowl, lip blunting reduces K_{ADD} at low-subsonic speeds. However, these data show that over 50% of the theoretical additive drag is not recovered. It seems reasonable for K_{ADD} to tend toward 1.0 at $MFR = 0$, where the inlet is essentially a flat plate. Values of K_{ADD} at high MFR are highly dependent upon inlet contours.

The pressure model of Fig. 9, which employed NACA series 1 cowls, shows excellent additive drag cancellation at low speeds. The results indicate that, using this lip design, complete cancellation should be obtained at mass-flow-ratios above about 0.6, which should be about as low as any inlet, even one sized for VTOL, will have to operate. Even at lower mass-flow-ratios, K_{ADD} does not get above about 0.2.

The two-dimensional wedge supersonic inlet that was studied is shown in Fig. 10. Results of K_{ADD} tests are also plotted in this figure and are summarized in Fig. 11. The model was a force model of the entire aircraft. There was no lip pressure instrumentation. The inlet was an external compression, vertical-wedge, two-ramp design with a control system that held the normal shock just in front of the inlet lip. The first ramp was fixed at 6°, and the second could be varied from $-2.75°$ to $+16°$ relative to the first ramp (net turning angle varies from 3.25° to 22°). The control schedule called for the second ramp to assume the $-2.75°$ position ($\theta = 3.25°$) for flight between 0 and 1.2 Mach and to be programed with Mach number from this point up to 16° ($\theta = 22°$) at Mach 2.0. In curve a, K_{ADD} is seen to vary in an erratic manner with both Mach number and mass-flow-ratio for the $-2.75°$ position of the second ramp. Significantly, the values are high (between 0.5 and 0.9). If this aircraft is

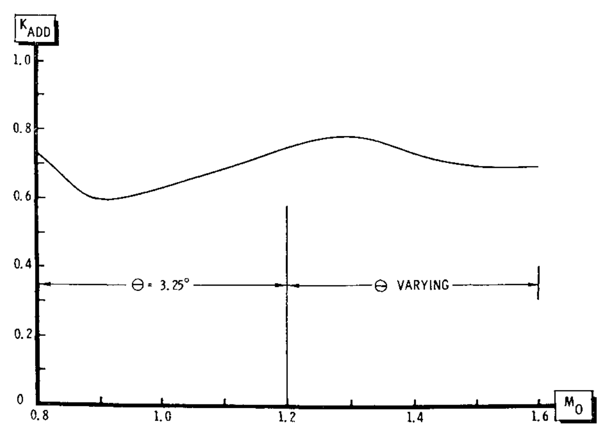

Fig. 11 Mach 0.80–1.60 K_{ADD} summary curve. Two-dimensional ramp inlet. NA-64-363.

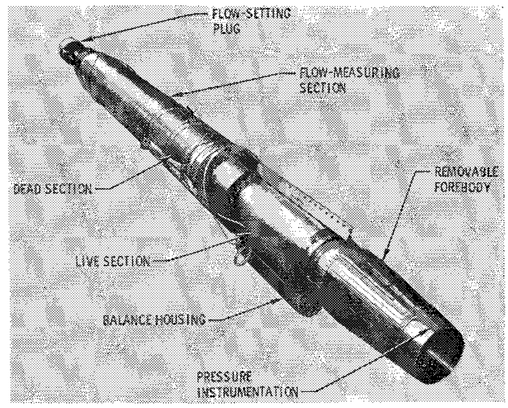

Fig. 12 Additive drag test model.

to have good transonic penetrating capability, considerable attention should be paid to finding a way to reduce these values. In curve b, K_{ADD} is seen to be significantly lower for the lower net turning angle. However, for a given engine airflow demand, D_{ADD} might be greater for the lower turning angle. Thus, the net turning angle must be optimized such that the product ($D_{ADD} \times K_{ADD}$) is a minimum. Finally, this drag figure should be traded against the bypass drag that would result if the mass-flow-ratio were increased to reduce D_{ADD} for the optimized turning angle. A K_{ADD} summary curve for this two-dimensioned inlet is presented in Fig. 11 where the curve shown would be representative of a realistic ramp schedule.

Model Program

With the inadequacies of the existing data established, a completely new test program was initiated to provide more authoritative design information for inlet optimization. The initial base-point series of tests was run in mid-July 1964 at Mach numbers from 0.3 to 1.25 for a group of pitot inlets.[11] Further testing is contemplated for two-dimensional supersonic inlets in the near future, with the possibility of adding some hypersonic configurations later.

The model (Fig. 12) consists of a basic flow-measuring afterbody with a variable plug for controlling mass-flow-ratio. At low Mach numbers, suction is applied to achieve high MFR points. A shielded external drag balance is used to measure forebody drag, the live forebody being supported from the dead afterbody via the balance assembly. The live and dead portions are sealed with a 16-element labyrinth seal. Pressures in the seal region are measured and accounted for in the final data. The universal rear section of the forebody accommodates a variety of inlet front sections, which together with the flow-measuring afterbody were used for all the tests. Six nose inlet configurations, shown in Fig. 13, were fabricated for the model, although, because of available test time, only five

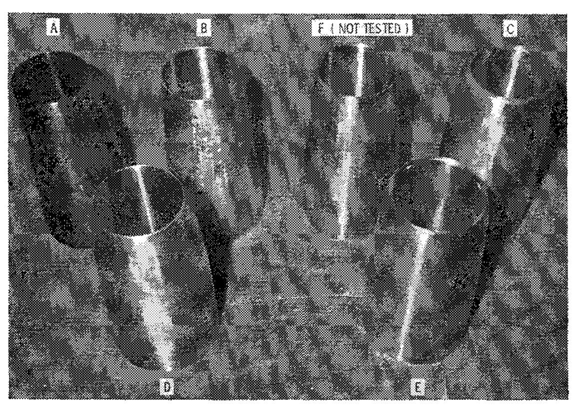

Fig. 13 Interchangeable open nose inlets for test model.

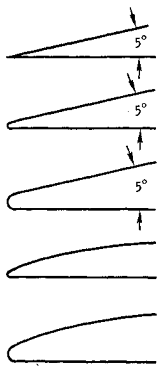

COWL	LIP RADIUS (IN)	r/D_{LE}	D_{MIN}/D_{MAX}	X/D_{MAX}
A	0	0	0.692	1.846
B	0.050	0.011	0.692	1.846
C	0.250	0.050	0.692	1.846
D	0.050	0.011	0.692	1.846
E	0.250	0.050	0.692	1.846

Fig. 14 Lip profiles for test inlet configurations (Note: Cowls *D* and *E* externally contoured to conform to NACA Series 1 contour).

were tested. Two of the five inlets, designated *D* and *E*, were externally contoured to conform to the basic NACA Series 1 cowl. These two differed in that the *D* cowl had a 0.050-in. internal lip radius, whereas the *E* cowl had an internal lip radius of 0.250 in. The *A*, *B*, and *C* cowls consisted of 5° conical cowls with varying amounts of bluntness. The *A* cowl had a sharp lip, and the *B* and *C* cowls had leading-edge radii of 0.050 and 0.250 in., respectively. Figure 14 shows the lip profiles for each of the tested inlet configurations.

Each inlet cowl was extensively instrumented with pressure taps, thereby enabling K_{ADD} determination to be made from both force balance and static pressure measurements.

The total pressure recovery of the inlets is measured incidental to measuring the momentum of the internal air at the exit of the live section. In the present test series, recovery was of little importance, being essentially 100% in all of the subsonic cases and normal shock recovery in the low-supersonic cases. For more sophisticated supersonic and hypersonic inlets, changes in lip, ramp, side-plate, or spike design to reduce K_{ADD} may have an effect on recovery which must be considered in arriving at a final performance figure.

Testing at a given Mach number involved merely a stepwise variation of mass-flow-ratio. Data reduction was carried out in the manner described for the data obtained from the literature.

Some of the correlated K_{ADD} data from this model program are given in Fig. 15. The data presented are for each of the five tested inlets at Mach 0.3, 0.6, 0.9, and 1.27. The NACA Series 1 contoured inlets, *D* and *E*, yielded significantly lower K_{ADD} values than the 5° conical inlets with minor lip blunting. K_{ADD} values for cowl *C* (conical cowl with r/D_{LE} = 0.050), however, compared favorably with cowls *D* and *E*, particularly in the low-subsonic Mach range. Of interest is the fact that cowl *E* shows complete cancellation of the theoretical additive drag (i.e., K_{ADD} = 0) at Mach 0.285 at mass-flow-ratios greater than 0.6 and nearly complete cancellation in the high *MFR* range at Mach 0.585.

Concluding Remarks

The data shown indicate that careful lip contouring and lip blunting can greatly reduce the effect of the theoretical additive drag on the performance of aircraft equipped with pitot inlets. For strictly subsonic aircraft, the best cowl design is probably a NACA-1 contour with some lip bluntness. Cowl *C* of Fig. 15 shows performance close to a NACA-1 design, particularly at low-subsonic Mach numbers.

For subsonic/transonic aircraft, a pitot inlet with a NACA Series 1 external contour and a slight amount of blunting, such as cowl *D* of Fig. 15, would give the best cancellation of theoretical D_{ADD} at normal mass-flows and at high-subsonic Mach numbers.

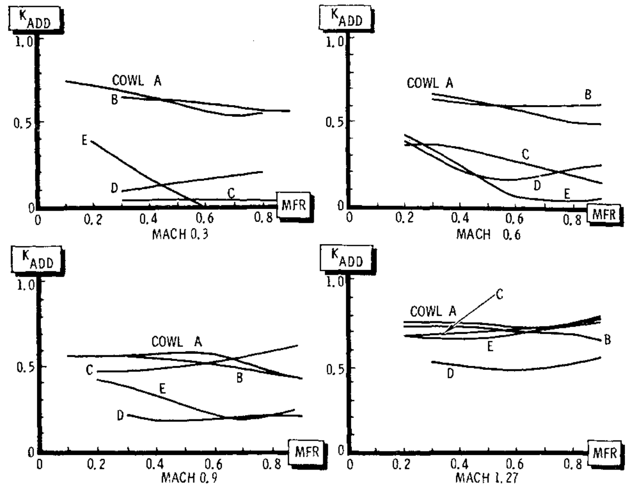

Fig. 15 Mach 0.30–1.27 North American Aviation tests. Pitot inlet. Effect of lip blunting and external contouring.

Applying best estimates of K_{ADD} (from the curves of Figs. 8, 9, and 15) to the supersonic and V/STOL transport vehicles results in the actual physical drag levels indicated by the asterisks in Figs. 4 and 5. The existing data indicate that, for the subsonic V/STOL transport, theoretical additive drag will impose hardly any penalty on performance.

For the supersonic transport, on the other hand, there remains a large drag penalty during subsonic cruise and transonic acceleration. The effect of the transonic acceleration penalty is to decrease supersonic range about $1\frac{1}{2}$% for a 3000 mile mission (over the range that would result with K_{ADD} = 0). For shorter missions, the percent reduction would be larger. The effect on subsonic range is far more significant, as is indicated in Fig. 6.

References

[1] Fradenburgh, E. A. and Wyatt, D., "Theoretical performance of sharp lip inlets at subsonic speeds," NACA/Lewis Rept. 1193 (1954).

[2] Randall, L. M., "Importance of air induction system design to supersonic aircraft," Society of Automotive Engineers National Aerospace Meeting, Los Angeles, Calif. Paper 586B (October 1962).

[3] Kuchemann, D. and Weber, J., *Aerodynamics of Propulsion* (McGraw-Hill Book Co., Inc., New York, 1953).

[4] Pearson, L. W., "Theoretical and experimental transonic additive drag," North American Aviation, Los Angeles Div. NA-64-363 (April 1964).

[5] Sibulkin, M., "Theoretical and experimental investigation of additive drag," NACA/Lewis Rept. 1187 (1954).

[6] Baals, D. D., Smith, N. F., and Wright, J. B., "The development and application of high critical-speed nose inlets," NACA/Langley Rept. 920 (1948).

[7] Randall, L. M., Haagenson, W. R., and Kavanagh, P., "Experimental investigation to determine the effect of several design variables on the performance of the F-100 duct inlet," North American Aviation, Los Angeles Div. NA-53-26 (January 1953).

[8] Mossman, E. A. and Anderson, W. E., "The effect of lip shape on a nose-inlet installation at Mach numbers from 0 to 1.5 and a method for optimizing engine-inlet combinations," NACA/Ames RMA54B08 (May 1954).

[9] Klein, H., "The calculation of the scoop drag for a general configuration in a supersonic stream," Douglas Co., Santa Monica Div. SM-13744 (April 1950).

[10] Blackaby, J. R. and Watson, E. C., "An experimental investigation at low speeds of the effects of lip shape on the drag and pressure recovery of a nose inlet in a body of revolution," NACA/Ames TN3170 (April 1954).

[11] Petersen, M. W. and Tamplin, G. C., "Open nose inlet additive drag test results at subsonic and transonic speeds," North American Aviation, Los Angeles Div. NA-64-921 (October 1964).